

CHAPTER 111

THE SWASH ZONE: A FOCUS ON LOW FREQUENCY MOTION

Adam M. Shah¹ and J. William Kamphuis²

ABSTRACT

This paper presents an analysis of physical model tests of the swash zone. A mild, impermeable slope was used to create a wide swash zone. Bichromatic and irregular waves with varying wave heights, wave periods and wave grouping were tested. The experiments showed the swash zone to be dominated by low frequency motions, which were closely related to the incident wave groups. The incident waves were still grouped in the surf and swash zones.

An empirical relationship was determined, relating the long wave height at the shoreline to the deep water wave parameters. The long waves were found to be partially reflected from the swash zone and this partial reflection was successfully simulated by the superposition of an absorbed and a reflected long wave. The generation of spurious long waves and the seiche at the natural frequency of the equipment were also investigated.

INTRODUCTION

The swash zone extends from the limit of run-down to the limit of run-up. Although the very shallow water and the low incident wave energy levels in the swash zone might suggest it to be of minor importance, Kraus *et al.* (1981) and Kamphuis (1991) have shown that it contains a peak in sediment transport rate. Thus the swash zone plays an important role in shaping natural beaches. Since very little is known about flow in the swash zone, all the numerical models of beach morphology use drastic simplifications within the swash zone. The goal of this paper is, therefore, to improve the understanding of swash zone flow so that eventually the computation of beach morphology can be improved.

Wave energy in the swash zone is concentrated in the infra-gravity band, at frequencies about one order lower than the incident waves. These low frequency motions are initially generated offshore by the distribution of wave

¹ MSc, Research Assistant, Dept. of Civil Engineering, Queen's University, Kingston, Ontario, Canada, K7L 3N6.

² Professor of Civil Engineering, Queen's University, Kingston, Ontario, Canada, K7L 3N6, kamphuis@civil.queensu.ca.

heights within wave groups. A Bound Long Wave travels with the incident waves at their group velocity and with its trough located under the highest waves in the group (Longuet-Higgins and Stewart, 1964).

Inshore of the break-point, the behaviour of the long waves and their interaction with individual breakers is not fully understood. One theory states that the bound long wave shoals as it travels inshore. Upon reaching the breakpoint it becomes a free long wave which is reflected seaward once it reaches the shore (Longuet-Higgins and Stewart, 1964). Another theory suggests that the amplitude of long waves decreases from the break-point and if the breaking is gentle all of the long wave energy is absorbed along with the short wave energy (Ottesen - Hansen *et al.*, 1980). Symonds *et al.* (1980) present a completely different mechanism for long waves within the surf zone. They state that the long wave motion inside the breaker zone is driven by the spatial variation of the breakpoint. As the breakpoint location varies with the group frequency it generates a long wave at that frequency. The experimental results in this paper favour a modified Longuet-Higgins and Stewart (1964) approach.

The long waves inside the breaking zone are difficult to study in the field. But they are also difficult to study in the laboratory, where studies of long waves are plagued by undesired low frequency motions resulting from spurious long waves coming off the wave generator and from seiche. Most wave generators are driven by a signal that only generates the grouped short waves and does not generate the bound long wave that accompanies the wave groups. Since the bound long wave will physically accompany the short waves anyway, this simplistic wave generation procedure amounts to generation of a spurious, free long wave equal and opposite to the bound long wave, travelling at the shallow water wave speed. Seiche (an oscillation at the natural frequency of the laboratory flume) results from transfer of wave energy into the natural frequency band of the wave flume. Such an oscillation increases with time and may eventually dominate the low frequency motion, contaminating measurements. Since the predominant mode of oscillation for the natural frequency has an antinode at the shoreline, seiche has the greatest significance in shallow water. Flick and Guza (1980) developed an expression for the natural frequency of the first mode of oscillation for a composite section, consisting of a slope and a horizontal section:

$$\sigma_n = \frac{1}{4} \pi \frac{(g\beta x_s)^{1/2}}{x_L + x_s} \quad (1)$$

where β is the slope, x_s is the length of the slope and x_L is the total length of the flume.

In view of the confusion and lack of understanding of long wave motion and the difficulties in studying long waves in the field and in the laboratory, this study (described in more detail in Shah, 1996) has the following objectives:

1. To relate the long wave at the shoreline to the offshore wave climate by a simple expression,
2. To study the development of the long wave from the breakpoint to the swash zone,
3. To study the contamination of long wave measurements by incorrect wave generation and seiche.

EXPERIMENTAL PROCEDURE

Laboratory tests were conducted at the Queen's University Coastal Engineering Research Laboratory (QUCERL) and the National Research Council of Canada (NRCC). An impermeable 0.6 m wide ramp with a 1:50 slope was installed in a 2.1 m wide wave flume at QUCERL. The mean water depth at the wave generator was 0.7 m, 26.2 m from the still water line (Figure 1). The tests at NRCC were conducted in a larger facility and made use of their more sophisticated generators. The ramp in Figure 1 was extended by 5 m, at NRCC, increasing the test depth to 0.80 m. The distance from the wave generator to the toe of the ramp was also increased from 1.2 m to 5 m.

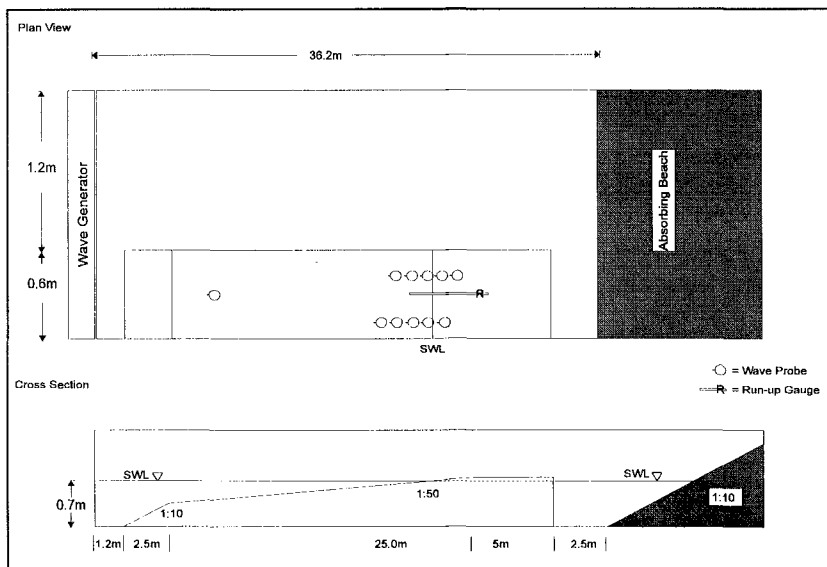


Figure 1 Experimental Setup at QUCERL

Table 1 summarizes the test series. For the irregular waves, H_s is the offshore significant wave height, T_p the peak period, and GF the groupiness factor (Funke and Mansard, 1979). For the bichromatic waves, H_1 and H_2 are the wave heights of the two components, T_{av} , the average period and T_g the group period.

Table 1 Wave Parameters Tested

Irregular Waves 19 tests at QUCERL 16 tests at NRCC			Bichromatic Waves 24 tests at NRCC			
H_s	T_p	GF	H_1	H_2	T_g	$T_{av.}$
.08 to .175 m	0.83 to 2.0 s	0.5 to 1.0	.05 to .25 m	.015 to .10 m	14 to 38 s	1.7 to 1.9 s

The effect on swash flow was measured at QUCERL by 11 capacitance wave gauges placed between 1.7 m offshore of the still water line and 0.5 m inshore. As well, a continuous run-up gauge was placed in the swash zone. At NRCC, 12 probes were placed between the breakpoint and the shoreline, to detect shoaling of the long waves and decay of the breakers through the surf zone.

The principal tool for data reduction was spectral analysis. Since all of the wave spectra showed a minimum spectral density at about one half the incident peak frequency, this was used to separate the high frequency and low frequency components. Wave heights were calculated as the zero spectral moment H_{moh} , for the high frequency ($f \geq f_p/2$) and H_{mol} , for the low frequency ($f < f_p/2$) components.

RESULTS

Swash Zone Wave Measurements

The QUCERL experiments provided high resolution measurements of water surface elevation within the swash zone. Figure 2 presents the first 50 seconds of sampling for four of the wave signals from an irregular wave test in which the initial conditions were $T_p=1.00$ s, $H_0=0.116$ m, $GF=0.94$. The heavy line is a low pass filtered signal to identify the long wave action. The low pass cut-off frequency was $f_p/2 = 0.50$ Hz. The importance of the low frequency motion ranges from minor at the offshore probe to near-total domination at the still water line.

The first panel shows the unbroken wave train for the furthest probe offshore. The groupiness of the wave train is clearly visible. In the second panel, Probe 1 was located 1.7 m offshore of the still water line, in the inner surf zone, and the wave train shows the saw-tooth profile indicative of broken waves. Though the waves are well inshore of the breakpoint they are still highly grouped and a high proportion of the incident waves are still intact. The final two panels show waves within the swash zone and present the final stages of wave decay. There are substantially fewer individual waves in the swash zone than there are incident waves as breakers coalesce into less frequent, more energetic uprush surges. The rate of decay is not the same for all the breakers. The waves that arrive at the swash zone during a strong downrush, characterized by a steep drop in water level, decay rapidly. For example, those waves arriving between 27 and 34 seconds at Probe 1 never reach Probe 2, which is only 1.2 m closer to the

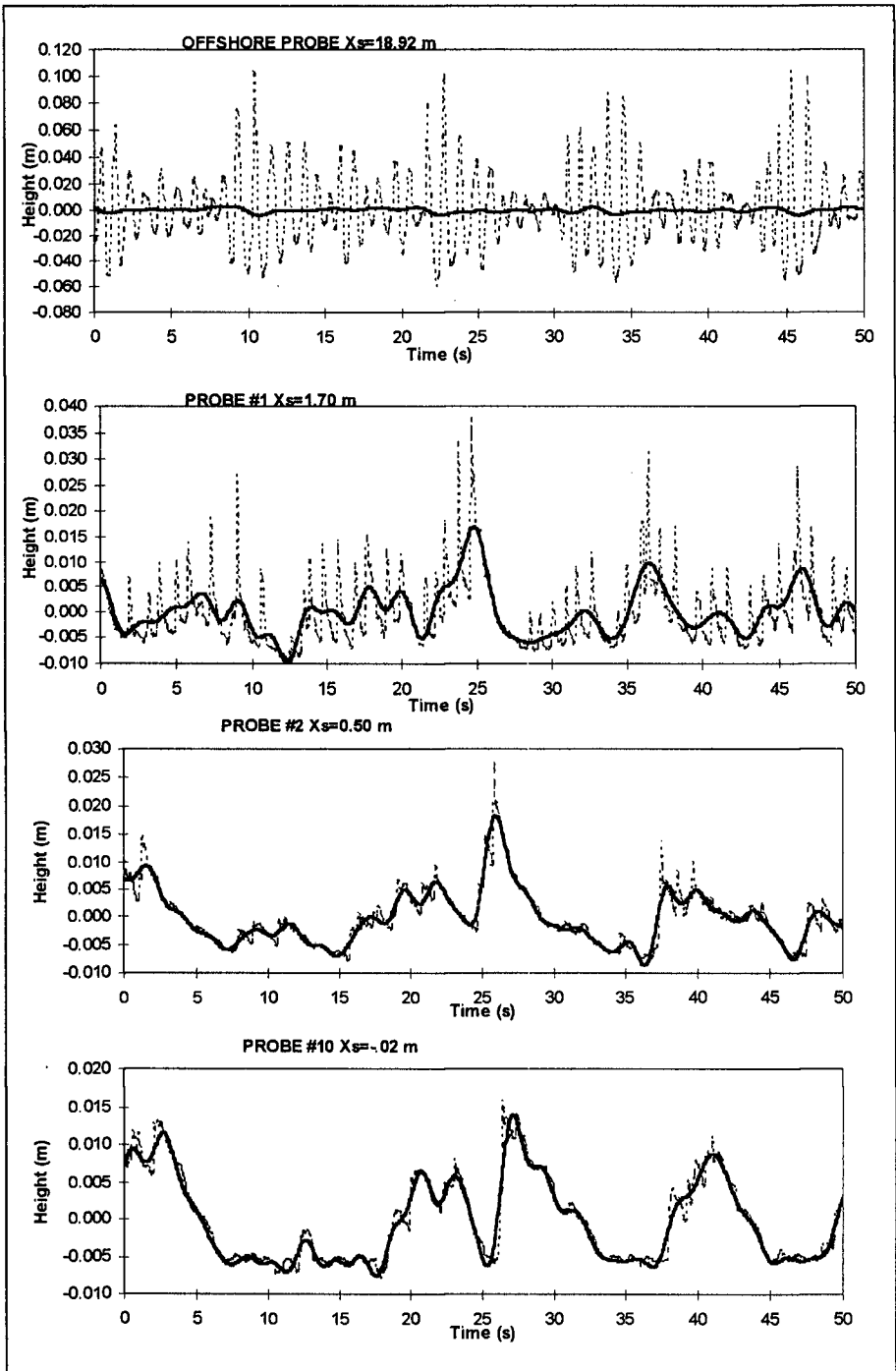


Figure 2 Example Wave Trains with Low-Pass Filtering

shoreline. Waves that arrive during an uprush cycle, for example from 20 to 25 s at Probe 1, progress with much less energy dissipation and eventually correspond to the extreme uprushes.

In addition to the increase in amplitude of the low frequency motion, the phase of the low frequency motion relative to the wave groups shifts 180° as the waves approach shore. At the offshore probe, the troughs of the low frequency motion occur under the highest waves in the group, at 2, 10 and 45 s. But at the probes inshore of the breakpoint, the highest waves in the group are on the crest of the long waves. This phase shift of the low frequency motion relative to the incident wave groups is undoubtedly complicated and no satisfactory explanation or theory has yet been proposed.

Spurious Long Waves and Seiche

Some of the tests at NRCC were specifically aimed at studying the effect of undesirable, spurious long waves resulting from not generating the bound long wave in the wave generation process. Such spurious long waves were found to be negligible for the tests conducted at NRCC due to a relatively large water depth at the wave generator and the longer wave period (Ottensen-Hansen *et al.*, 1980). For the tests at QUCERL such waves were calculated to contribute 10-15% to the total measured long wave energy.

Seiche was measured by recording water levels after the wave generator was shut down. The natural period of the NRCC flume was found to be 55 s, which is somewhat larger than the value of 40 s calculated from Equation (1). The difference can be attributed to run-up. Equation (1) predicts the resonant period based on the still water dimensions of the flume, as if vertical walls existed at the generator and the still water line. In the experiments, run-up excursions of 2.5 m or more were typical and the time required for the long wave to travel this distance is significant, since the speed of propagation is very small in very shallow water. The travel time required from the original still water line to the limit of run-up and back may be approximated using an expression developed by Wilson (1966) for the natural frequency of a triangular basin:

$$t = 1.64 \frac{2L}{\sqrt{gh}} \quad (2)$$

For a typical wave set-up of 20 mm at the shoreline and a run-up excursion of 2.5 m, the additional time is 19 s and when this is added to the value calculated by Equation (1) the total of 59 s, is close to the measured value of 55 s.

Contamination by the seiche was evaluated from the energy at the natural frequency and its harmonics. Bichromatic waves excited seiche, even during short duration testing. When the group frequency approached the natural frequency, energy leaked into the natural frequency band of the flume. Figure 3 shows the energy leakage for a bichromatic test with $H_1=0.10$ m, $H_2=0.05$ m, $T_g=38$ s. The offshore spectral peak, at $X_s = 9.8$ m, is at the group frequency of 0.026 Hz while

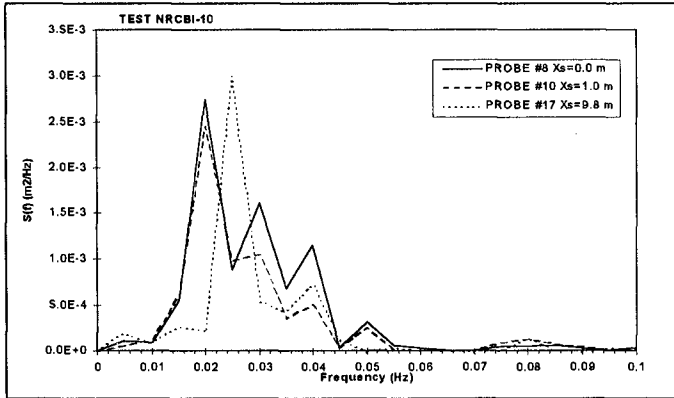


Figure 3 Energy Leakage from Group to Natural Frequency

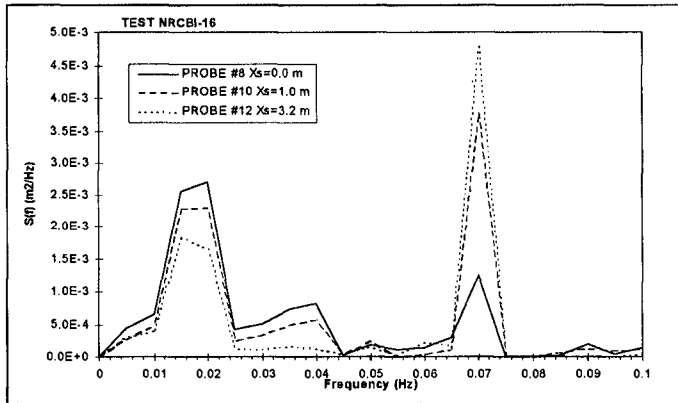


Figure 4 Subharmonic Excitement of the Natural Frequency

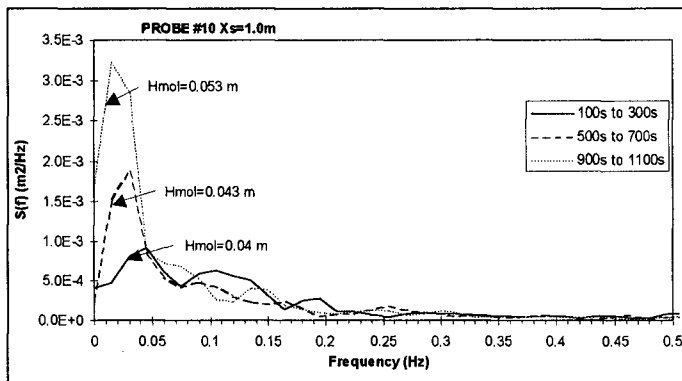


Figure 5 Build-up of Seiche Energy for Irregular Wave Testing

in the vicinity of the shoreline the spectral peak has shifted to the natural frequency of 0.018 Hz. Obviously the long wave measurements in this test were severely contaminated by seiche. Seiche was also generated when the group frequency matched a superharmonic of the natural frequency. Figure 4 shows a bichromatic wave test with $H_1=0.075$ m, $H_2=0.015$ m, $T_g=14$ s. The peak, at 0.07 Hz, is at the group frequency, the peak near 0.04 Hz is the first subharmonic and the peak near 0.018 Hz is the second subharmonic, which is also the natural frequency of the flume.

Irregular wave tests built up energy at the natural frequency over a longer duration; short duration tests did not excite appreciable seiche. Irregular waves have a broad band of group frequencies and can excite the natural frequency by a first-order interaction between any two incident group frequencies. Figure 5 presents three long wave spectra calculated at different times for the same irregular wave test with $H_o=0.175$ m, $f_p=0.5$ Hz, $f_g=0.05$ Hz. While the energy levels at and above the group frequency of 0.05 Hz were relatively constant, energy levels near the natural frequency of .02 Hz increased by a factor of six. This resulted in an incorrect increase of the calculated long wave H_{mo} from 0.04 m to 0.053 m.

Swash Zone Long Wave Height

The long wave height at the shoreline, $H_{mol,s}$ is a function of the beach slope and the deep water zero moment wave height, H_o , wave length, L_o , and Groupiness Factor. The effect of beach slope was not tested. One dimensionless expression that was found to satisfy the necessary conditions is:

$$\frac{H_{mol,s}}{L_o} = 0.078 \left(\frac{H_o}{L_o} \right)^{0.7} \quad (3)$$

It is based on the 31 irregular wave tests that were not contaminated by seiche and is shown in Figure 6. The correlation coefficient, r^2 is 0.81 and the different symbols represent ranges of groupiness. A consistent trend with groupiness is not apparent. This is, most likely because the calculation of the Groupiness Factor was affected by the reflected long wave at the offshore probe.

Long Wave Reflection Model

The cross-shore profiles of long wave height, H_{mol} , with distance offshore showed partial nodes and antinodes (the solid triangles in Figure 7). This indicates the long waves may be simulated by superimposing a reflected and absorbed long wave component. Thus, the Longuet-Higgins and Stewart (1964) development, suitably modified using partial long wave reflection is needed to explain the experimental results.

The fully reflected component was simulated by the solution presented in Lamb's (1932) for the reflection of a long wave over a sloping bottom. The height

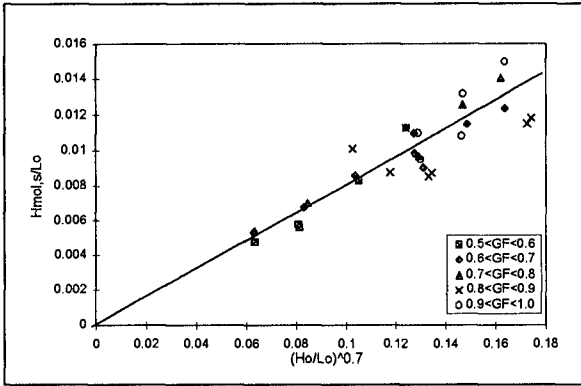


Figure 6 Regression Results for All Irregular Wave Tests

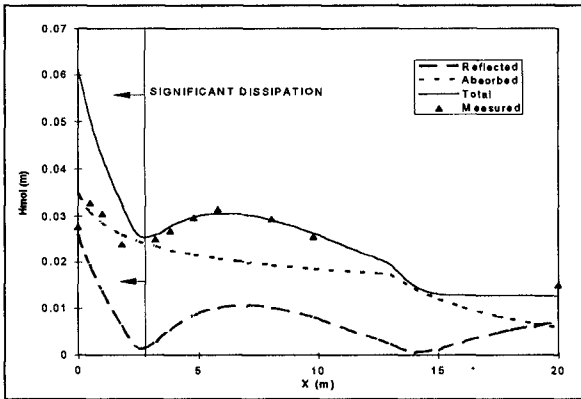


Figure 7 Example Model Results for Bichromatic Wave Test

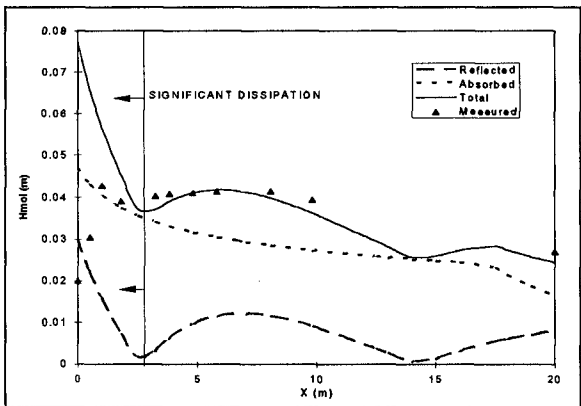


Figure 8 Example Model Results for Irregular Wave Test

of the standing wave envelope, ζ_r , is twice the absolute value of Lamb's Bessel function solution,

$$\zeta_r = 2\zeta_{r,s} \left| J_0 \left(\sqrt{\frac{4\sigma^2 x}{g\beta}} \right) \right| \quad (4)$$

where ζ_r is the local reflected long wave height, $\zeta_{r,s}$ is the reflected long wave height at the shoreline, J_0 is the zero order Bessel function, σ is the angular frequency of the long wave, g is the acceleration due to gravity, β is the beach slope and x is the distance offshore of the still water line. The reflected long wave is shown as the dashed line in Figure 7.

The absorbed portion of the long wave energy shoals as it travels inshore; the dotted line in Figure 7. Prior to breaking, the shoaling of the short waves will increase the height of the bound long wave. Theoretically this rate has been shown to vary with depth according to $h^{-3/2}$ by Longuet-Higgins and Stewart (1964). They assume, however, that the depth varies slowly enough that the shoaling long wave attains equilibrium. In practice the depth probably changes too rapidly for the long wave to reach equilibrium. Typically the distance from the wave generator to the breakpoint was less than one wavelength of the bound long wave and hence the actual shoaling rate was considerably smaller than $h^{-5/2}$. Since the focus of this research was on the swash zone, few probes were placed in the outer surf zone and for most tests the offshore probe was the only measured point on the bound long wave shoaling profile. Thus, a precise quantification of the bound long wave shoaling rate was not possible from these results.

If it is assumed that the bound long wave becomes a free long wave upon breaking, Green's Law, which states that the wave height of a free long wave varies with depth according to $h^{-1/4}$, can be used inside the breaker. The transition from bound to free long wave shoaling should begin where breaking is initiated. The present model assumes an abrupt transition between the two shoaling rates at the onset of breaking, as estimated using the criteria of Kamphuis (1991). This is an over-simplification; the transition is more gradual and will occur over the width of the breaking zone.

In very shallow water, wave set-up contributes to the effective depth and must be included. Theoretically, wave set-up increases linearly from the maximum set-down at the breakpoint to maximum set-up at the shoreline (Longuet-Higgins and Stewart, 1964). This relationship was a good approximation to the actually measured values of set-up. Thus, the local absorbed long wave height, ζ_a , inshore of the breaking point for a coordinate system with its origin at the still water line may be expressed, using a combination of wave set-up and wave shoaling according to Green's Law as:

$$\zeta_a = \zeta_{a,s} \left(\frac{h_o + \bar{\eta}_b + (\bar{\eta}_s - \bar{\eta}_b) \left(1 - \frac{h_o}{h_b}\right)}{\bar{\eta}_s} \right)^{-1/4} \quad (5)$$

where ζ_a is the local absorbed long wave height, $\zeta_{a,s}$ is the absorbed long wave height at the shoreline, h_o is the local still water depth, h_b is the breaking depth, $\bar{\eta}_s$ is the set-up at the shoreline and $\bar{\eta}_b$ is the set-down at the breakpoint. Offshore of the breaker

$$\zeta_a = \zeta_{a,s} \left(\frac{h_b + \bar{\eta}_b}{\bar{\eta}_s} \right)^{-1/4} \left(\frac{h_o}{h_b} \right)^{-k} \quad (6)$$

where k is the shoaling rate for the bound long wave (equal to $5/2$ if the depth is changing very slowly).

Superimposing the wave reflection analyzed from Equation (4) on Equations (5) and (6) produced Figure 7, a prediction of the local long wave height, representing the partially reflected standing wave system for a linear long wave over a sloping bottom, in the absence of losses:

$$\zeta_t = \zeta_a + \zeta_r \quad (7)$$

The model can calculate the long wave height profile if $\zeta_{a,s}$, $\zeta_{r,s}$, and σ are known. Figure 7 compares the results of the model (solid line) with measured data for a bichromatic wave test with $H_1 = 0.1$ m, $H_2 = 0.05$ m, $T_{av} = 1.9$ s, $T_g = 18$ s; the reflected and absorbed components are respectively the dashed and dotted lines. The predicted long wave profile, offshore of the first partial node, matches the observed standing wave pattern well. Inshore of this node, (at approximately $X = 2$ m), the model overpredicts the measured H_{mol} profile severely. This is because energy dissipation removes energy from the long wave system, since the extremely shallow depths make bottom friction significant. The measured profile peaks at about 1 m offshore and then abruptly decreases. Figure 8 shows similar results for an irregular wave test with $H_o = 0.175$ m, $T_p = 0.5$ Hz, $GF = 0.9$. More long wave energy is absorbed in the irregular wave test (Figure 8) than in the bichromatic wave test (Figure 7), which translates into less reflection. This may be due to the broad-bandedness of the irregular wave group frequency.

Comparable results to Figures 7 and 8 were obtained for all 15 of the 24 bichromatic tests and the 9 irregular tests at NRCC which were not contaminated by seiche.

Long wave height at the shoreline was represented by a simple empirical expression (Equation 3).

Long waves are partially reflected from within the swash zone. A model was developed that predicts the shape of the observed partial standing long wave envelope by adding the absorbed and reflected long waves (Equations 4-7). These equations take into account shoaling.

Seiche at the natural frequency of the basin was found to be a much more important laboratory effect in contaminating long wave experiments than the spurious long waves off the generator. Bichromatic tests were found to be contaminated by the seiche, when the group period approached the natural period of the flume or its superharmonics. Irregular wave tests were only contaminated when longer test durations were used.

Acknowledgments

This study was funded by the operating grants programme of the National Sciences and Engineering Research Council. The assistance of Etienne Mansard and the facilities provided by the National Research Council of Canada Hydraulics Laboratory are greatly appreciated. The funding for Adam Shah to attend ICCE '96 was provided by the Queen's University School of Graduate Studies.

References

- Flick, R.E. and Guza, R.T. (1980), "Paddle Generated Waves in Laboratory Channels," *Journal of the Waterway, Port, Coastal and Ocean Div.*, ASCE, Vol. 106, pp. 79-97.
- Funke, E.R. and Mansard, E.P.D. (1979), "On the Synthesis of Realistic Sea States," National Research Council of Canada, *Hydraulics Laboratory Technical Report*, LTR-HY-66.
- Kamphuis, J.W. (1991), "Incipient Wave Breaking" *Coastal Eng.*, Vol 15, pp. 185-203.
- Kraus, N.C., Farinto, R.S. and Horikawa, K. (1981), "Field Experiments on Longshore Sand Transport in the Surf Zone," *Coastal Engineering in Japan*, Vol. 24, pp. 171-194.
- Lamb, H. (1932), "*Hydrodynamics*," 6th Edition, Cambridge University Press, p. 738.
- Longuet-Higgins, M.S. and Stewart, R.W. (1964), "Radiation Stresses in Water Waves, a Physical Discussion, with Applications," *Deep Sea Res.*, Vol. 11, pp. 529-564.
- Ottensen - Hansen, N.E., Sand, S.E., Lundgren, H., Sorensen, T. and Gravesen, H. (1980), "Correct Reproduction of Group Induced Long Waves," *Proc. 17 Intl. Conf. Coastal Eng.*, Sydney, ASCE, pp. 784-800.
- Shah, A.M. (1996), "*The Swash Zone: A Focus on Low Frequency Motion*", M.Sc. Thesis, Queen's University, 138 pp.
- Symonds, G., Huntley, D.A. and Bowen, A.J. (1982), "Two Dimensional Surf Beat: Long Wave Generation by a Time Varying Breakpoint," *J. Geophys. Res.*, Vol. 87, pp. 492-498.
- Wilson, B.S. (1966), "Seiche", in *Encyclopedia of Oceanography*, R.W. Fairbridge ed., Academic Press, New York.